

## Transport properties across the $\text{La}_{2/3}\text{Ca}_{1/3}\text{MnO}_3/\text{SrTiO}_3$ heterointerface

LI. Balcells,<sup>1</sup> LI. Abad,<sup>1</sup> H. Rojas,<sup>1,2</sup> A. Perez del Pino,<sup>1</sup> S. Estrade,<sup>3</sup> J. Arbiol,<sup>3,4</sup> F. Peiro,<sup>3</sup> and B. Martinez<sup>1,a)</sup>

<sup>1</sup>Institut de Ciència de Materials de Barcelona, Campus Universitari de Bellaterra, E-08193 Bellaterra, Spain

<sup>2</sup>Escuela de Física, Facultad de Ciencias, Universidad Central de Venezuela, Apdo. 20513, Caracas 1020-A, Venezuela

<sup>3</sup>EME/CerMAE/IN<sup>2</sup>UB, Dept. d'Electrònica, Universitat de Barcelona, c/ Martí Franques 1, 08028 Barcelona, Spain

<sup>4</sup>TEM-MAT, Serveis Científicotècnics, Universitat de Barcelona, c/ Martí Franques 1, 08028 Barcelona, Spain

(Presented on 9 November 2007; received 6 September 2007; accepted 26 October 2007; published online 6 February 2008)

The transport properties across  $\text{La}_{2/3}\text{Ca}_{1/3}\text{MnO}_3/\text{SrTiO}_3$  (LCMO/STO) heterostructures with different thicknesses of the STO insulating barrier have been studied by using atomic force microscopy measurements in the current sensing (CS) mode. To avoid intrinsic problems of the CS method we have developed a nanostructured contact geometry of Au dots. The conduction process across the LCMO/STO interface exhibits the typical features of a tunneling process. The analysis of  $I(V)$  curves by using the Simmons model allows us to determine the barrier height ( $\varphi_0 \approx 0.6$  eV) of STO barriers. © 2008 American Institute of Physics. [DOI: 10.1063/1.2833760]

Complex oxides have attracted much interest recently because they show a broad spectrum of intrinsic functionalities that allow envisaging the development of a new generation of oxide-based electronic, magnetic, and magnetoresistive devices.<sup>1,2</sup> Among them manganese perovskites occupy a prominent place due to their very peculiar properties, such as the colossal magnetoresistive response and the half metallic character. Nevertheless, the successful implementation of oxide-based devices requires preserving bulklike magnetic and transport properties at surfaces and interfaces. Thus, the physics and chemistry of surfaces and interfaces become a subject of primary interest since they can drastically modify magnetic and electronic properties reducing the performances of thin films and multilayered structures due to chemical inhomogeneity, strain, charge transfer, or spin exchange interactions.<sup>3,4</sup>

Interfacial effects are especially relevant in manganite-based magnetic tunneling junctions where not only electronic but also magnetic properties are important. Due to the strong orbital-lattice coupling lattice strain effects may be very important in manganites<sup>5</sup> thus, playing a relevant role on the degradation of the magnetic properties.<sup>6</sup> However, other causes, such as polar discontinuity across the interface, may also be important.<sup>7</sup> In this sense, recent theoretical studies predict the appearance of electronic phase segregation with the formation of a spin- and orbital-ordered insulator phase at the manganite-insulator interface due to the reduction of carriers at the interface.<sup>8</sup>

In this work we have carefully analyzed the transport properties across  $\text{SrTiO}_3$  (STO) insulating barriers on top of  $\text{La}_{2/3}\text{Ca}_{1/3}\text{MnO}_3$  (LCMO) films at room temperature by using atomic force microscopy (AFM) working in the current

sensing (CS) mode. To avoid intrinsic problems of the CS method we have developed a nanostructured contact geometry of Au dots. The conduction process across the LCMO/STO/Au heterostructure exhibits the typical features of a tunneling process. The analysis of  $I(V)$  curves by using the Simmons model allows us to determine the barrier height,  $\varphi_0 \approx 0.6$  eV, in good agreement with previous reports for STO tunneling barriers.

LCMO epitaxial thin films of about 60 nm thick have been grown by rf sputtering on top of (001) STO substrates [ $T_D=800$  °C and a pressure of 330 mTorr (Ar+20% O<sub>2</sub>)].<sup>9</sup> Substrates have been treated previous to deposition selecting a TiO<sub>2</sub> atomic termination.<sup>10</sup> The LCMO growth process is of two-dimensional layer by layer type at first stages but then it changes to a three-dimensional type, therefore, the atomic termination of the LCMO layer is not determined. Insulating STO layers of different thickness  $t$  ranging from about 1 to 3 nm have been grown on top of the LCMO films using the same growth conditions. Metallic contacts have been prepared by *ex situ* deposition of a 30 nm thick Au dots on top of the samples by e-beam evaporation at room temperature. Finally, different nanostructured contact geometries have been defined by using a nanostencil shadow mask.<sup>11</sup>

Structural characterization of the samples has been performed by x-ray diffraction, AFM, and high resolution transmission electron microscope. The samples exhibit high crystalline quality with the STO(001)/LCMO(001)/STO(001) epitaxial relationship and with sharp interfaces. In Fig. 1 we show a high resolution image of a cross section to illustrate the nanostructural quality of the samples. Surface roughness of LCMO/STO bilayers turns out to be very small (rms  $\approx 0.2$  nm) and steps of about 0.4 nm corresponding to one unit cell are clearly visible [see Figs. 2(a) and 2(b)].

The transport properties across the LCMO/STO interface have been measured by means of AFM system working on

<sup>a)</sup>Electronic mail: ben.martinez@icmab.es

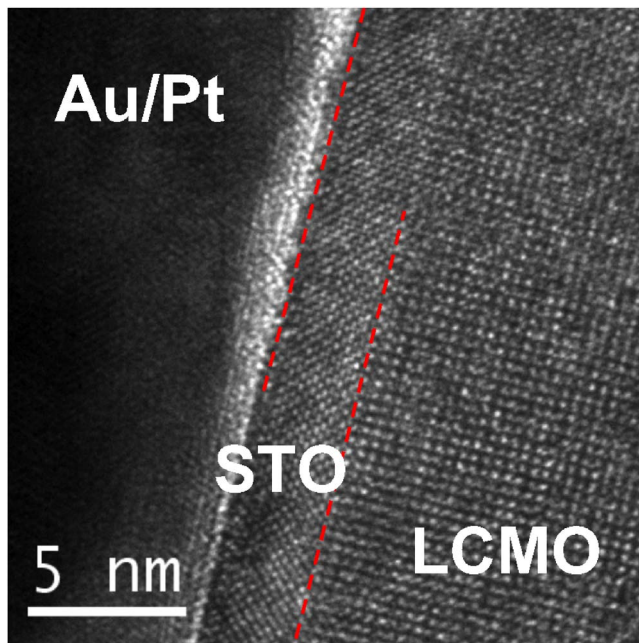


FIG. 1. (Color online) High resolution TEM images of the LCMO/STO/Au interface.

the CS mode with a silicon tip coated with a boron doped diamond conducting film. Transport measurements across a ferromagnetic oxide/insulating barrier bilayers by direct contact of the doped diamond tip with the sample surface are very difficult to do due to the strong dependence on the effective contact area.<sup>12</sup> Without a very accurate study and control of the mechanisms involved in the tip-surface interaction, not always controllable, a strong dependence on the unreliable contact area is found as evidenced by variations of conductivity mimicking the subjacent topography of the films [see Fig. 2(c)].  $I(V)$  curves taken at different points of the surface exhibit the typical features of a tunneling conduction process but with very high dispersion.

To avoid those problems related with the variation of the effective contact area we have developed a nanostructured contact geometry by *ex situ* deposition of a 30 nm thick Au layer using a nanostencil shadow mask. By using this proce-

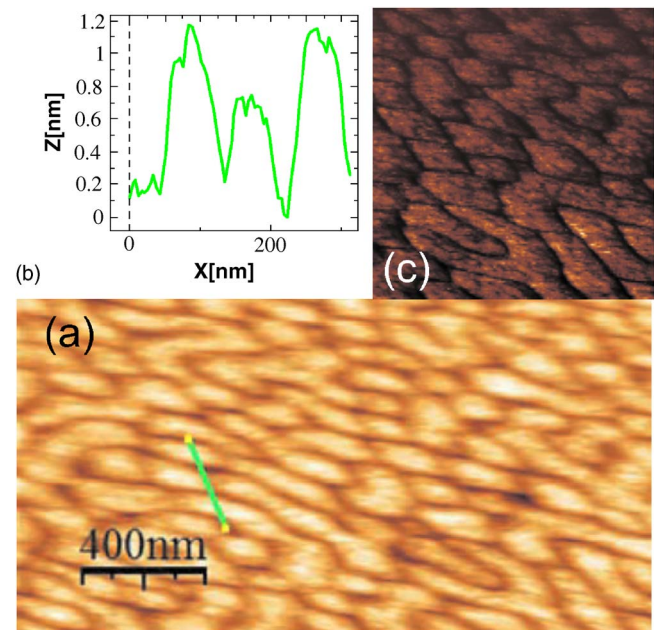


FIG. 2. (Color online) (a) AFM topography of STO/LCMO/0.8 nm STO film. (b) Profile along the green line on (a) to show the smoothness of the STO surface. (c) Current map for the same sample (white color corresponds to saturated current, 10 nA) measured by direct contact of the AFM tip with the STO insulating layer.

dure gold dots with diameters ( $\phi$ ) ranging from few hundred nanometers to some micrometers have been fabricated. In Fig. 3 we show the topography and the profile of one of the Au dots (a) and the conductivity map (b) of a set of these Au nanostructures. As expected, the conduction through the LCMO/STO/Au heterostructure exhibits the typical features of a tunneling process (see Fig. 4). Characteristic  $I(V)$  curves measured by placing the AFM tip at different points on top of the Au dots give completely equivalent results in contrast with the dispersion observed when  $I(V)$  curves are measured by direct contact between the AFM, tip and the STO surface. Even more,  $I(V)$  curves measured in Au dots with different diameters exhibit a perfect scaling as a function of the Au dot area. Therefore, it can be concluded that a homogeneous current injection through the Au/STO/LCMO heterostructure

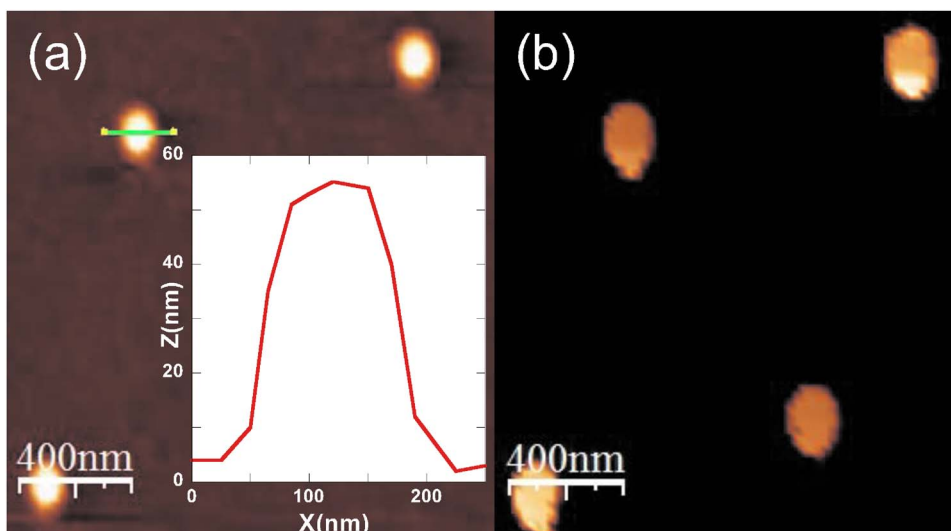


FIG. 3. (Color online) (a) AFM topography for a sample with Au contact dots of  $\phi \approx 160$  nm. The profile of one of the Au dots is shown. (b) Current map of the same sample showing high conductance on the Au dots and insulating character outside the dots.

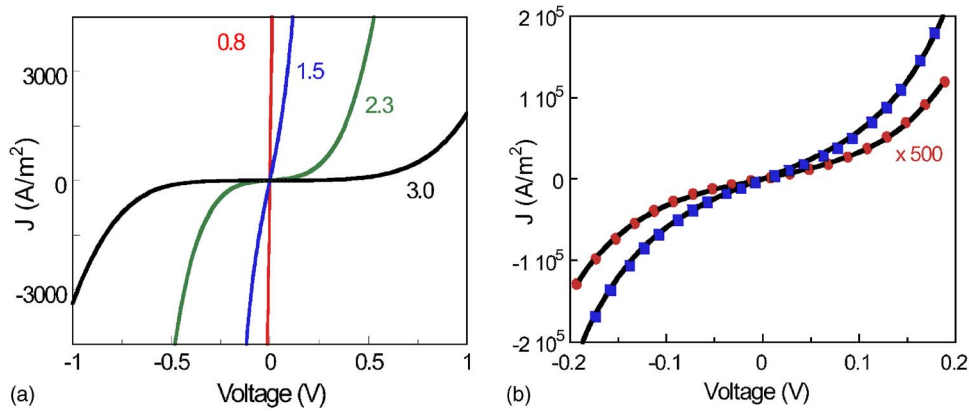


FIG. 4. (Color online) (a)  $J/V$  curves at room temperature for samples with different STO barrier thicknesses (in nm) by using a constant Au dot size ( $\varnothing \approx 800$  nm). (b) Some examples of the fitting of the  $I(V)$  curves by using the Simmons model in the intermediate voltage regime. The fits correspond to samples with STO barrier thickness of  $t=0.8$  nm (■) and  $t=2.3$  nm (●).

has been achieved and that the current injected through the STO/LCMO interface is independent of the AFM tip effective contact area, being determined by the size of the Au dot. By controlling the size of the Au dots, we are able to measure resistances down to  $\sim 10^4 \Omega$ , that will be considered as the lower limit of our experimental setup.

We have studied the transport properties across de LCMO/STO interfaces as a function of the thickness of the insulating STO barrier. In Fig. 4(a) we show the  $J(V)$  characteristic curves for different barrier thicknesses. It is found that  $J(V)$  curves are strongly dependent on the barrier thickness  $t$ . The  $J(V)$  characteristic curves have been analyzed by using the Simmons model at the intermediate -voltage range to estimate  $\varphi_0$  (barrier height) and  $S$  (barrier thickness).<sup>13</sup>

The fits of the  $J(V)$  curves corresponding to samples with different STO thickness barriers have been performed in the voltage range of  $\pm 0.2$  V. Some examples of these fits are shown in Fig. 4(b). The barrier height between LCMO and STO is given by  $\varphi_0 = W_{\text{LCMO}} - \phi_{\text{STO}}$  being  $W_{\text{LCMO}}$  the work function of LCMO [ $\approx 4.8$  eV (Ref. 14)] and  $\phi_{\text{STO}}$  being the electron affinity of STO [ $\approx 3.9$  eV (Ref. 15)], thus in the present experimental conditions the barrier height should be smaller than  $\sim 0.9$  eV. It is worth mentioning the concordance between samples with different barrier thicknesses giving a value of the barrier height  $\varphi_0 \approx 0.6$  eV in agreement with the estimation of the barrier height given above. This value of  $\varphi_0$  is also in good agreement with previous values reported by Sun *et al.* for STO tunnel barriers in LSMO/STO/LSMO heterostructure<sup>16</sup> and slightly larger than those reported in Ref. 12.

In summary, we have carefully measured and analyzed the transport properties across the LCMO/STO heterostructures by using AFM working in the CS mode. To overcome intrinsic problems related to the determination of the actual contact area between the AFM tip and the surface, we have developed a nanostructured contact geometry of Au dots. With this experimental setup a homogeneous current injection across the LCMO/STO interface is accomplished with the current density being controlled by the Au dot area. The conduction across the LCMO/STO heterostructure exhibits the typical features of a tunneling process. The analysis of

$I(V)$  curves by using the Simmons model allows us to determine the barrier height,  $\varphi_0 \approx 0.6$  eV, in good agreement with previous reports of STO tunneling barriers. This method allows an easy characterization of insulating barriers for the fabrication of oxide-based tunneling junctions.

We acknowledge financial support from Spanish MEC (MAT2006-13572-C02-01), CONSOLIDER (CSD2007-00041), FEDER Program and Generalitat de Catalunya (2005SGR-00509). H.R. wishes to acknowledge the partial support given by Venezuela research council FONACIT (S3-2006000683) during his stay at ICMAB. We also would like to express our deepest gratitude to Dr. F. Pi (LCP-UAB) and M. J. Gonzalez (PCB-UB) for technical support and Dr. A. F. Lopeandia (GNAM-UAB) for interesting discussions.

<sup>1</sup>H. Koinuma, *Thin Solid Films* **486**, 2 (2005).

<sup>2</sup>N. Tsuda, K. Nasu, A. Fujimori, and K. Siratori, *Electronic Conduction in Oxides* (Springer-Verlag, Berlin, 2000).

<sup>3</sup>M. Izumi, Y. Ogimoto, Y. Okimoto, T. Manako, P. Ahmet, K. Nakajima, T. Chikyow, M. Kawasaki, and Y. Tokura, *Phys. Rev. B* **64**, 064429 (2001).

<sup>4</sup>M. Izumi, Y. Murakami, Y. Konishi, T. Manako, M. Kawasaki, and Y. Tokura, *Phys. Rev. B* **60**, 1211 (1999).

<sup>5</sup>A. J. Millis, T. Darling and A. Migliori, *J. Appl. Phys.* **83**, 1588 (1998); Z. Fang, I. V. Solov'yev, and K. Terakura, *Phys. Rev. Lett.* **84**, 3169 (2000).

<sup>6</sup>Ll. Abad, V. Laukhin, S. Valencia, A. Gaup, W. Gudat, Ll. Balcells, and B. Martínez, *Adv. Funct. Mater.* **17**, 3918 (2007).

<sup>7</sup>W. A. Harrison, E. A. Kraut, J. R. Waldrop, and R. W. Grant, *Phys. Rev. B* **18**, 4402 (1978).

<sup>8</sup>L. Brey, *Phys. Rev. B* **75**, 104423 (2007).

<sup>9</sup>S. Valencia, L. Balcells, J. Fontcuberta, and B. Martínez, *Appl. Phys. Lett.* **82**, 4531 (2003).

<sup>10</sup>G. Koster, B. L. Kropman, A. J. H. M. Rijnders, D. H. A. Blank, and H. Rogalla, *Appl. Phys. Lett.* **73**, 2020 (1998).

<sup>11</sup>A. F. Lopeandia, J. Rodríguez-Viejo, M. Chacón, M. T. Clavaguera-Mora, and F. J. Muñoz, *J. Micromech. Microeng.* **16**, 965 (2006).

<sup>12</sup>M. Bibes, M. Bowen, A. Barthélémy, A. Anane, K. Bouzehouane, C. Carrétero, E. Jacquet, J.-P. Contour, and O. Durand, *Appl. Phys. Lett.* **82**, 3269 (2003); K. M. Lang, D. A. Hite, R. W. Simmonds, R. McDermontt, D. P. Pappas, and J. M. Martinis, *Rev. Sci. Instrum.* **72**, 2726 (2004).

<sup>13</sup>J. G. Simmons, *J. Appl. Phys.* **34**, 2581 (1963).

<sup>14</sup>D. W. Reagor, S. Y. Lee, Y. Li, and Q. X. Jia, *J. Appl. Phys.* **95**, 7971 (2004).

<sup>15</sup>J. Robertson, *J. Vac. Sci. Technol. B* **18**, 1785 (2000).

<sup>16</sup>J. Z. Sun, L. Krusin-Elbaum, P. R. Duncombe, A. Gupta, and R. B. Laibowitz, *Appl. Phys. Lett.* **70**, 1769 (1997).